STUDIA UBB CHEMIA, LXX, 2, 2025 (p. 179-190)
(RECOMMENDED CITATION)
DOI:10.24193/subbchem.2025.2.12

THE EFFECT OF SYNTHESIS PROCESS PARAMETERS ON THE PHYSICO-CHEMICAL PROPERTIES AND PHOTOCATALYTIC ACTIVITY OF PRISTINE AND ZrO_2-DOPED TiO_2 CATALYSTS

Marija VASİĆ JOVEV[a,*], Radomir LJUPKOVİĆ[a], Katarina STEPİĆ[a], Marjan RANĐELOVİĆ[a], Miloš MARINKOVİĆ[b], Aleksandra ZARUBİCA[a,*]

ABSTRACT. In this study, TiO_2-based catalysts were synthesized using a modified sol-gel method. The catalysts were prepared at two different pH values (10 and 13) and were subsequently doped with zirconia to improve their photocatalytic performance. The physico-chemical properties of the catalysts, including structural, textural, morphological, and thermal properties, were studied using XRD, BET, SEM, and TG/DTA methods, respectively. The photocatalytic activity of the synthesized catalysts was tested in the degradation/decolorization reaction of methylene blue dye. The results indicated that the synthesis parameters and zirconia doping had a significant impact on the catalysts' physico-chemical characteristics and, therefore, their activity. It can be pointed out that catalysts with improved properties and enhanced photocatalytic activity can be obtained by carefully selecting and optimizing synthesis conditions, as well as by modifying or doping them with a suitable dopant.

Keywords: *TiO_2, ZrO_2-doping, Photocatalysis*

INTRODUCTION

One of the major challenges confronting modern society and a significant issue for researchers is water pollution [1]. Organic pollutants, such as dyes commonly used in industry, can lead to severe environmental problems [1, 2, 3].

---

[a] *Department of Chemistry, Faculty of Science and Mathematics, University of Niš, Serbia*
[b] *Institute of General and Physical Chemistry, University of Belgrade, Belgrade, Serbia*
[*] *Corresponding authors: marija.vasic@pmf.edu.rs, marijavasic84@gmail.com; zarubica2000@yahoo.com*

Many of these pollutants are toxic and carcinogenic [3, 4]. They can reduce sunlight penetration in water, disrupt photosynthesis [1, 4], and harm aquatic life and marine organisms [1]. Therefore, it is crucial to remove these pollutants from wastewater before discharging it into the environment [1, 2, 3]. Organic dyes are commonly used in various industries, including textiles, paper, printing, and paint [1, 2], with methylene blue (MB) dye being frequently studied in research [1, 2, 3]. Over the years, numerous methods and techniques have been studied to remove organic pollutants from water and wastewater [3, 4].

One often-tested method is heterogeneous catalysis, with TiO_2-based materials being extensively researched. TiO_2 is a semiconductor that generates electrons and electron holes in its conduction and valence bands, respectively, when exposed to UV light [2]. Despite its numerous advantages and exceptional photocatalytic properties [2], TiO_2 has certain limitations. Due to its wide band gap, TiO_2 can only be activated by UV radiation and has a rapid recombination of electron charge carriers [2]. To overcome these limitations, numerous methods and techniques have been studied, including doping or modifying with different metals such as noble metals (Ag, Au, Pt, Pd, etc.) [4-8], alkaline-earth metals (such as Mg) [9], or transition metals (Fe, Cu, Mo, W, Zr, etc.) [1, 10-14].

Moreover, various process parameters during catalyst synthesis (such as the pH of the preparation solution, the applied calcination temperature, etc.) can significantly influence the catalyst's structural, textural, morphological, and other properties [10, 15-19]. These parameters can be adjusted to design materials with preferable physico-chemical properties, thus influencing their photocatalytic activity.

In this study, two different TiO_2-based catalysts were prepared using the sol-gel method, with two pH values (10 and 13) adjusted during the preparation process as parameters that can affect the physico-chemical properties and photocatalytic activity of the TiO_2-based samples. The resulting catalysts were subsequently modified/doped with zirconia as a dopant [10]. Zirconium was selected as a dopant because its ionic radius (Zr^{4+}) is similar to the ionic radius of Ti^{4+}. This similarity suggests the potential for the substitution and/or deformation of Ti with Zr in the crystal lattice of TiO_2. Additionally, the formation of crystal defects could occur, promoting better and prolonged separation of charge carriers (electrons and holes) and enhancing photocatalytic efficiency [10, 20-22].

In this study, we investigated the physico-chemical characteristics, crystal structure, morphology, textural, and thermal properties of the prepared catalysts using various techniques. Additionally, we examined the photocatalytic activity of all synthesized catalysts in the photocatalytic reaction of methylene blue dye decolorization/degradation under relatively mild reaction conditions (low-energy UV irradiation and the original pH value of the model solution).

The results presented in this paper indicate that different process parameters during material synthesis, as well as the doping with the selected dopant, significantly influenced the physico-chemical characteristics and photocatalytic activity of the prepared catalysts.

As previously mentioned, this study employed sol-gel and wet impregnation methods to synthesize pristine TiO_2 and zirconia-doped TiO_2-based catalysts with optimized physico-chemical properties. To the best of our knowledge, no prior research has addressed the identical synthesis and modification methods for preparing pristine and zirconia-doped TiO_2-based catalysts using the same mass ratio, synthesis conditions, and precursors, while specifically focusing on the influence of the same synthesis process parameters, such as varying selected pH levels, on the properties and activity of the catalysts. Additionally, this study investigates the decolorization of MB dye under specific, relatively mild (low-energy) conditions using the prepared catalysts.

RESULTS AND DISCUSSION

Structural properties

The structural properties of the prepared TiO_2-based and ZrO_2-doped TiO_2 catalysts are shown in Figure 1 [10].

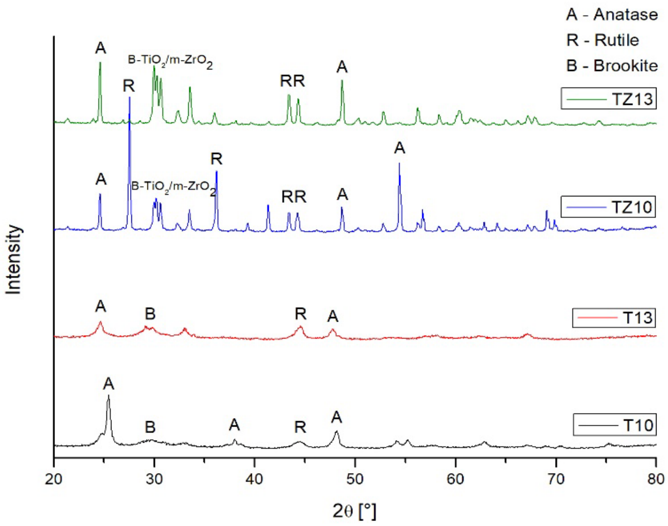

Figure 1. XRD patterns of: T10, T13, TZ10, and TZ13 catalysts (A - Anatase, B - Brookite, R - Rutile)

The results presented in Figure 1 indicate that the T10 catalyst is predominantly characterized by an anatase (A) crystalline phase, with the highest intensity peak at around 25.5° (JCPSD Card No. 21-1272) [10, 23, 24]. Additionally, the initial formation of the rutile (R) crystalline phases has been detected (JCPDS 21-1276) [10, 24, 25], (and/or brookite (B)), indicating that the transformation from the anatase to rutile phase began at the applied calcination temperature of 550 °C [10].

Sample T13, synthesized at pH 13 and calcined at the same temperature, has a smaller proportion/volume of the anatase crystal phase compared to sample T10 (Figure 1). However, sample T13 shows an increased volume of the rutile crystal phase and a noticeable presence of the brookite crystal phase, which is present in a much smaller amount in sample T10. Additionally, the increase in pH from 10 to 13 resulted in a decrease in crystallite grain size. Namely, the estimated anatase crystal grain size for the T10 sample, calculated by Scherrer's equation, was approximately 20 nm, while the grain size for the T13 sample was around 15 nm [10]. Furthermore, sample T13 exhibited poorly defined low-intensity peaks, while sample T10 is characterized by well-defined intense peaks, indicating that the T10 catalyst has a more favorable crystal structure. Overall, the variation in pH during the synthesis process significantly influenced the structural properties of the prepared catalysts.

After doping with zirconia and calcination at 800 °C, the samples are characterized by sharper, stronger, and better-defined diffraction peaks. This indicates an increase in the crystallinity degree and an improved crystal structure. Furthermore, doping has resulted in increased crystallite sizes for both doped samples, measuring around 40 nm for the anatase crystal phase, compared to the pristine TiO_2 samples [10].

The sample TZ10 is characterized by a dominant crystalline phase of rutile (approximately 60%). This is expected at higher calcination temperatures, indicating that the phase transformation from anatase to rutile has occurred. In contrast, the doped TZ13 catalyst shows an increased presence of the anatase phase, which may be due to the presence of the dopant that can inhibit the anatase to rutile phase transformation. Additionally, the diffraction peak at 30° Bragg's angle is much more noticeable in TZ13 than in TZ10. This peak is believed to correspond to the brookite titania and/or monoclinic zirconia phase [10].

Textural properties

Nitrogen adsorption-desorption isotherm and pore size distribution curve for the modified TZ13 catalyst are presented in Figure 2 [10].

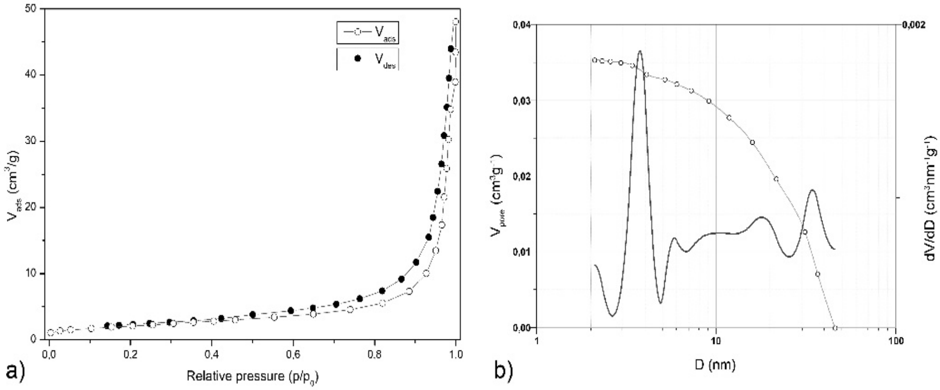

Figure 2. a) Nitrogen adsorption-desorption isotherm and b) pore size distribution curve for modified TZ13 catalyst [10]

Table 1. Textural properties of TZ13 catalyst [10]

Sample	S_{bet} (m^2/g)	Median pore size (nm)	Pore volume (cm^3/g)
TZ13	7.8	29.0	0.044

The nitrogen adsorption/desorption isotherm for catalyst TZ13, shown in Figure 2 a) [10], indicates the presence of mesopores. This sample is characterized by a type IV sorption isotherm with an H3 hysteresis type [10], according to the IUPAC classification of isotherms and hysteresis loops [26, 27]. The type of hysteresis observed suggests that the catalyst contains crack-shaped pores. Additionally, the relatively small specific surface area of the catalyst TZ13 (Table 1) aligns with the characteristics of the adsorption isotherms and the type of hysteresis loop. This may further affect the activity of the catalyst in photocatalytic reactions [10].

The results of the pore size distribution, as shown in Figure 2 b) [10], indicate that the catalyst TZ13 shows a non-standard bimodal, i.e., multimodal distribution of pores ranging between 3 and 40 nm. This confirms that TZ13 is mostly a mesoporous material. Most pores are near the micro-mesopore boundary (3-4 nm). Additionally, there is a noticeable presence of mesopores with a medium pore diameter of approximately 35 nm, although they are present in a somewhat smaller quantity/amount [10].

Morphological properties

The results of the morphological properties of the prepared TiO_2-based and ZrO_2-doped TiO_2 catalysts are shown in Figure 3 [10].

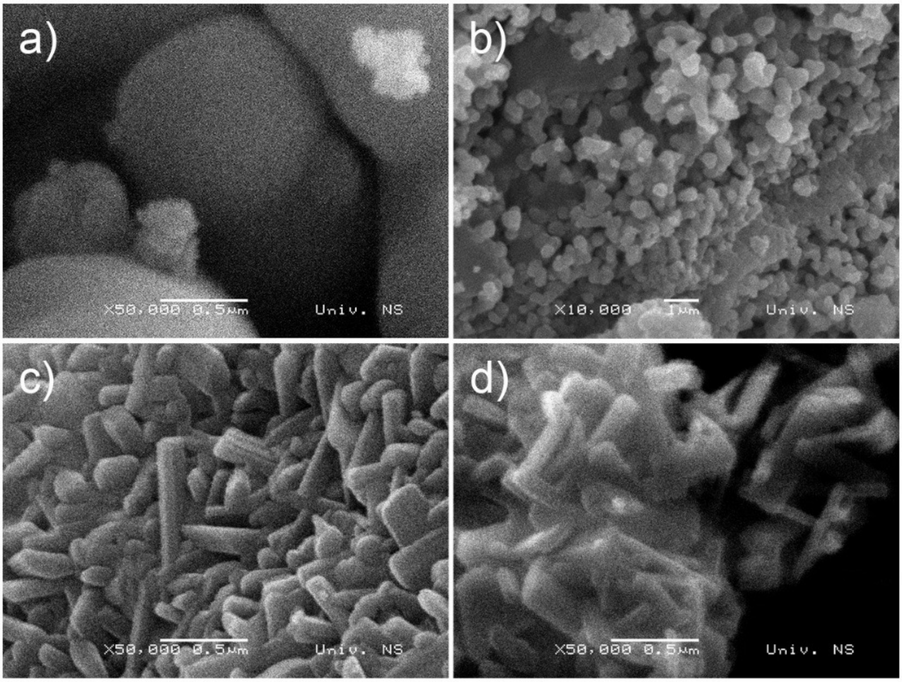

Figure 3. SEM micrographs of a) T10 (at x 50000 magnification), b) T13 (at x 10000 magnification), c) TZ10 (at x 50000 magnification), and d) TZ13 (at x 50000 magnification) [10]

The morphology of the T10 catalyst is characterized by agglomerated secondary particles that are around 100 nm in size and spherical in shape, along with inter-agglomerate pores. Some primary particles can also be observed, either in spherical or irregular shapes [10].

The high pH value of the medium used during the synthesis of catalyst T13 resulted in a significant change in the system's porosity and morphology. Namely, catalyst T13 displayed the formation of agglomerates or aggregates larger than 100 nm in size, and a decreased porosity, indicating a less favorable morphology for the material [10].

Based on the SEM results presented in Figures 3 c) and d), the doping process and the application of relatively high temperatures led to a significant change in the surface morphology of the doped catalysts, TZ10 and TZ13, compared to the pristine TiO_2-based catalysts. It can be noted that agglomerated secondary particles were formed in both doped samples due to the sintering process at the elevated calcination temperature. These agglomerates consist of irregular or rod-shaped primary particles that are larger than those in the pristine TiO_2-based catalysts, which aligns with the XRD results [10].

Thermal properties

The thermal properties of the prepared TiO_2-based and ZrO_2-doped TiO_2 catalysts are presented in Figure 4, which includes both DTA and TG analyses [10].

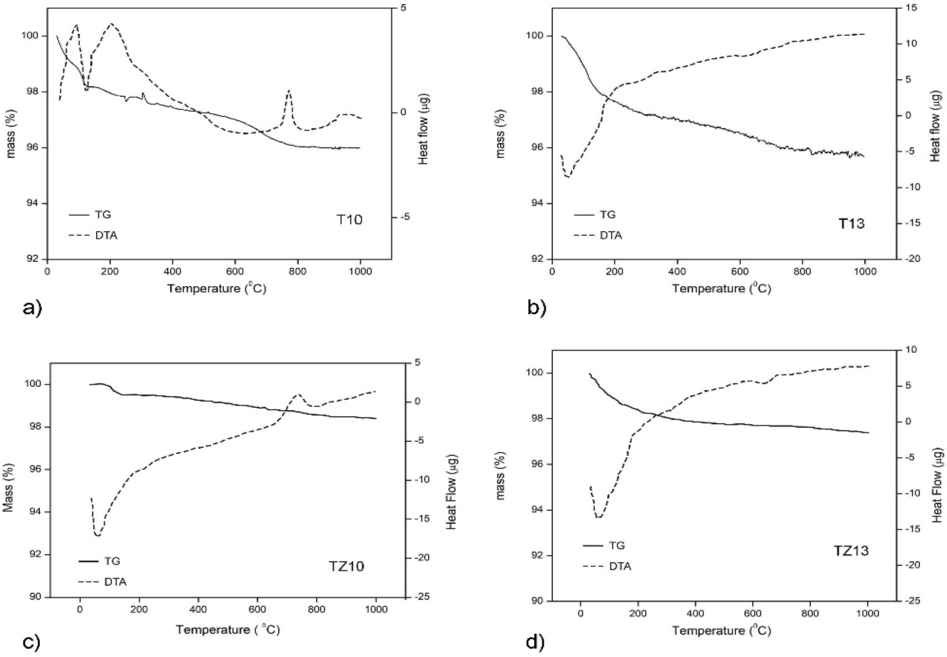

Figure 4. Thermal analysis of: a) T10, b) T13, c) TZ10, and d) TZ13 catalysts

The DTA curve for the T10 sample (Figure 4 a)) displays an endothermic effect occurring at around 120 °C. This effect correlates with a mass loss of up to 4%, as confirmed on the TG curve. This mass/weight reduction is ascribed to the removal of surface physisorbed water molecules or the evaporation of residual organic solvents during the drying process of catalyst preparation. Additionally, an exothermic peak observed at a temperature of 750°C indicates that the phase transformation from anatase to rutile shift towards higher temperatures, which aligns with the obtained results for structural properties. The DTA results for the T13 sample also showed an endothermic effect at approximately 100°C, followed by a mass loss of 4-5%, as shown in the TG curve (Figure 4 b)) [10].

Based on the results shown in Figures 4 c) and d), DTA curves indicate that both doped samples, TZ10 and TZ13, show an endothermic peak at approximately 100°C. This is followed by a mass loss of around 2-3%, as observed in the TG curves. This peak is attributed to dehydration, the removal of physisorbed water, and/or the evaporation of solvent and other remaining organic compounds present during the gel formation process in the synthesis of the catalysts. Additionally, the DTA curve for TZ10 shows an exothermic peak at approximately 750°C, which is most probably due to the presence and removal of constitutional water from residual hydroxide and/or phase transformation.

Photocatalytic activity

The photocatalytic activity of all the prepared catalysts in the degradation/decolorization of methylene blue dye is shown in Figure 5. It is important to note that the use of different pH values during the synthesis process, along with the addition of a dopant, significantly influences the physico-chemical properties of the catalysts, which subsequently affects their photocatalytic activity.

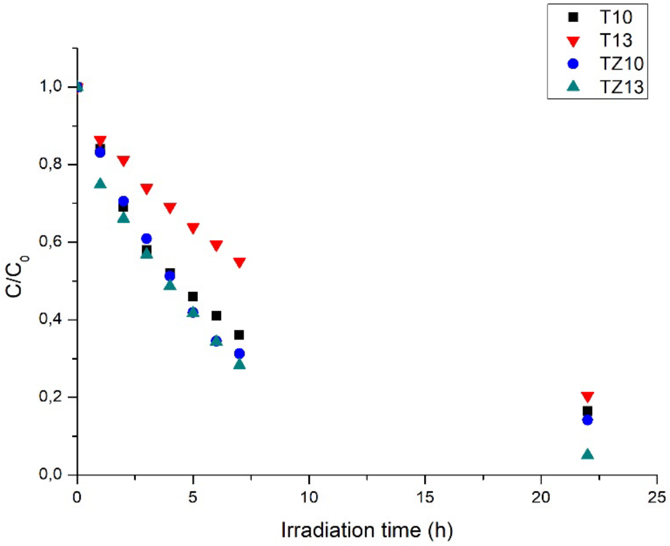

Figure 5. Photocatalytic degradation/decolorization of methylene blue dye with the use of T10, T13, TZ10, and TZ13 catalysts

When examining the pristine TiO_2-based samples, the T10 sample showed good activity in the photocatalytic reaction. Notably, the T10 sample exhibited a higher degradation rate than the T13 sample. This can be attributed to the more favorable structural (including better crystallinity, a dominant anatase crystalline phase, and an appropriate crystal grain size) and morphological properties of the T10 catalyst compared to the T13 sample.

Additionally, it is notable that doped sample TZ13 exhibited the highest photocatalytic activity among all the prepared samples. Despite having a relatively small specific surface area, this sample has a favorable mesoporosity, beneficial structural properties, and suitable morphology. As discussed earlier, sample TZ13 is characterized by good crystallinity and a dominant presence of the highly active anatase crystal phase, which is important for photocatalytic activity.

CONCLUSIONS

The modified sol-gel method was selected as a relatively simple method for preparing pristine and ZrO_2-doped TiO_2 catalysts. This study focuses on the influence of the synthesis process parameters (the use of two different pH values) on the physico-chemical properties and photocatalytic activity of the pristine and zirconia-doped TiO_2-based catalysts. The degradation/decolorization of methylene blue, carried out under relatively mild experimental conditions, was chosen to test the activity of all prepared samples. The results showed that both the pH during synthesis and the use of zirconia as a dopant significantly influenced the physico-chemical properties of the catalysts. As a result, both doped samples showed higher photocatalytic activity in the methylene blue degradation reaction compared to the pristine TiO_2 catalysts.

The TZ13 catalyst demonstrated the highest rate of degradation/ decolorization of methylene blue dye. This improved performance can be attributed to the dominant presence of the highly active anatase phase, along with an improved crystalline structure and the presence of mixed crystal phases (anatase, rutile, brookite titania, and/or monoclinic zirconia). Furthermore, the catalyst is characterized by beneficial mesoporosity, featuring bimodal or multimodal pore distribution and an appropriate surface morphology.

Overall, the findings in this paper highlight the importance of optimizing synthesis conditions and investigating suitable dopants to obtain efficient photocatalytic materials for future research focused on removing organic pollutants from water.

EXPERIMENTAL SECTION

In this study, four different catalysts were prepared: two catalysts based on pristine TiO_2 and two based on ZrO_2-doped TiO_2 catalysts. Firstly, TiO_2-based catalysts were synthesized using a modified sol-gel method, with Titanium isopropoxide as a precursor and a mixture of water and 2-Propanol for precipitation purposes. During the synthesis process, the pH value was varied and adjusted to 10 and/or 13 to obtain the two different catalysts. After precipitation, the samples were filtered and rinsed with deionized water and then with an alcohol/water mixture. Both TiO_2 samples were then dried at 105-110 °C for three hours. After drying, they were annealed at a temperature of 550 °C for three hours, with a heating rate of 10 °C per minute [10]. Samples prepared in this way were denoted as TX, where T stands for TiO_2 and X stands for the pH value used during the synthesis process (T10 and T13).

Subsequently, the prepared pristine TiO_2-based samples, T10 and T13, were modified/doped using the wet impregnation method. Both samples were doped using the same amount of $ZrOCl_2x8H_2O$ to obtain a mass ratio of 2.5 mass.% of zirconia. After doping, both doped samples were dried at 105 °C for three hours and then calcined at a temperature of 800 °C for three hours, with a heating rate of 10°C per minute [10]. Catalyst samples obtained in this way were denoted as TZX (TZ10 and TZ13), where T stands for TiO_2, Z stands for dopant ZrO_2, and X stands for used pH value used during the synthesis procedure, 10 or 13.

To determine the physico-chemical properties of the prepared catalysts, structural (XRD), textural (BET), morphological (SEM), and thermal (TG/DTA) analyses were performed [10]. Structural analysis (XRD) was performed on a Philips APD-1700 diffractometer in the 2θ range of 20-80° under the CuKα radiation source. The operation mode was set to 40 kV and 55 mA [10].

The average crystallite size (d) was calculated using the Scherrer equation (1) where k is the Scherrer constant, λ is the X-ray wavelength, β represents the peak at half maximum, and θ denotes the Bragg angle [10, 28]:

$$d = \frac{k\lambda}{\beta cos\theta} \tag{1}$$

The weight percentages of anatase and rutile were determined using the following equation by Spurr and Myers [29, 30]:

$$W_A = \frac{1}{1+1.265\frac{I_R}{I_A}} \tag{2}$$

where I_A and I_R are the intensities of the most intense peaks for anatase [101] and rutile [110] crystal phases, respectively.

Textural (BET) measurements were conducted using a Micromeritics ASAP 2010, based on the adsorption and desorption of liquid nitrogen, with helium as the carrier gas. Before measurements, all catalyst samples were degassed [10].

The morphology of the prepared catalysts was analyzed using a SEM JEOL JSM-6460LV scanning electron microscope (SEM) [10].

Thermal properties were determined using a Derivatograph MOM, M-1000 under static conditions, with temperatures ranging from 20 to 1000 °C. A heating rate of 10 °C/min and a cooling rate of 20 °C/min were applied [10].

The activity of the prepared TiO_2 and ZrO_2-doped TiO_2 catalysts was tested for the photocatalytic degradation/decolorization of methylene blue (MB) dye solution. To separate the adsorption process from photocatalysis, the prepared catalysts were placed in the dark with continuous stirring in the MB test solution for 24 hours. After the adsorption process was completed and the adsorption/desorption equilibrium was established, the photocatalytic reaction was carried out under UV illumination (using a UV lamp with a maximum emission at the wavelength 366 nm, 16W). Changes in the concentration of MB during both the adsorption and photocatalytic tests were monitored using a UV/VIS spectrophotometer.

ACKNOWLEDGMENTS

The work was supported by the Ministry of Science, Technological Development and Innovation of the Republic of Serbia (Contract numbers: 451-03-136/2025-03/200124, 451-03-137/2025-03/200124 and 451-03-136/2025-03/200051) and by the Ministry of Education, Science and Technological Development of the Republic of Serbia (Project number: ON 172061).

REFERENCES

1. H. Liyanaarachchi; C. Thambiliyagodage; C. Liyanaarachchi; U. Samarakoon; *Arab. J. Chem.,* **2023**, *16*, 104749.
2. L. Liu; Y. Liu; X. Wang; N. Hu; Y. Li; C. Li; Y. Meng; Y. An; *Appl. Surf. Sci.*, **2021**, *561*, 149969.
3. E. Basturk; M. Işık; M. Karatas; *Desalin. Water Treat.,* **2019**, *143*, 306-313.
4. C. H. Nguyen; C.-C. Fu; R.-S. Juang; *J. Clean. Prod.,* **2018**, *202*, 413-427.
5. D. Georgescu; Z. Pap; M. Baia; C.I. Fort; V. Danciu; G. Melinte; L. Baia; S. Simon; *Studia Universitatis Babes-Bolyai Chemia,* **2011**, *LVI*, 3, 51-58.
6. A. Peter; M. Baia; F. Toderas; M. Lazar; L.B. Tudoran; V. Danciu; *Studia Universitatis Babes-Bolyai Chemia*, **2009**, *LIV, 3*, 161-171.
7. R. Kumar; J. Rashid; M.A. Barakat; *Colloid. Interfac. Sci.,* **2015**, *5*, 1-4.
8. M. Khairy; E.M. Kamar; M.A. Mousa; *Mater. Sci. Eng. B-Adv.*, **2022**, *286*, 116023.
9. M. Giahi; D. Pathania; S. Agarwal; G.A.M. Ali; K.F. Chong; V.K. Gupta; *Studia Universitatis Babes-Bolyai Chemia*, **2019**, *LXIV, 1*, 7-18.

10. M. Vasić; *Optimisation and photocatalytic application of nanostructured* TiO_2*,* Doctoral Dissertation, Faculty of Sciences and Mathematics, University of Niš, Niš, **2017**.
11. C. Bathula; A. S Nissimagoudar; S. Kumar; A. Jana; S. Sekar; S. Lee; H.-S. Kim; *Inorg. Chem. Commun.,* **2024**, *164*, 112442.
12. A. Mishra; V. Verma; A. Khan; D. Kumar; T. S. Khan; V. Amoli; A. K. Sinha; *J. Environ. Chem. Eng.,* **2023**, *11*, 110319.
13. S. Bibi; S. S. Shah; F. Muhammad; M. Siddiq; L. Kiran; S. A. Aldossari; M. S. S. Mushab; S. Sarwar; *Chemosphere*, **2023**, *339*, 139583.
14. A. Khlyustova; N. Sirotkin; T. Kusova; A. Kraev; V. Titov; A. Agafonov; *Mater. Adv.,* **2020**, *1*, 1193.
15. M. Yalcin; *J. Cryst. Growth*, **2022**, *585*,126603.
16. R. Vasanthapriya; N. Neelakandeswari; K. Uthayarania; M. Chitra; *Dig. J. Nanomater. Bios.,* **2023**, *18*, 2, 767-771, https://doi.org/10.15251/DJNB.2023.182.767
17. A. Molea; V. Popescu; N. A. Rowson; A. M. Dinescu; *Powder Technol.,* **2014**, *253*, 22-28.
18. M. Lal; P. Sharma; C. Ram; *Optik*, **2021**, *241*, 166934.
19. N.C. Horti; M.D. Kamatagi; N.R. Patil; S.K. Nataraj; M.S. Sannaikar; S.R. Inamdar; *Optik*, **2019**, *194*, 163070.
20. J. Lukáč; M. Klementová; P. Bezdička; S. Bakardjieva; J. Šubrt; L. Szatmáry; Z. Bastl; J. Jirkovský; *Appl. Catal. B-Environ.,* **2007**, *74*, 83-91.
21. D. Kapusuz; J. Park; A. Ozturk; *J. Phys. Chem. Solids*, **2013**, *74*, 1026-1031.
22. M. Vasić; M. Randjelović; M. Momčilović; B. Matović; A. Zarubica; *Process. Appl. Ceram.,* **2016**, *10*, 189-198.
23. S.S. Arbuj; R.R. Hawaldar; U.P. Mulik; B.N. Wani; D.P. Amalnerkar; S.B. Waghmode; *Materials Science and Engineering B,* **2010**, *168*, 90-94.
24. W. Li; R. Liang; A. Hu; Z. Huang; Y.N. Zhou; *RSC Adv.,* **2014**, *4*, 36959.
25. R. Gao; Z. Jiao; Y. Wang; L. Xu; S. Xia; H. Zhang; *Chemical Engineering Journal,* **2016**, *304*,156-164.
26. K. Sing; D. Everett; R. Haul; L. Moscou; R. Pierotti; J. Rouquerol; T. Siemineiewska; *Pure Appl. Chem.,* **1985**, *57*, 603-619.
27. M. Thommes; K. Kaneko; A. V. Neimark; J. P. Olivier; F. Rodriguez-Reinoso; J. Rouquerol; K. S. W. Sing; *Pure Appl. Chem.,* **2015**, *87*, 1051-1069.
28. S.A. Hassanzadeh-Tabrizi; *J. Alloy. Compd.,* **2023**, *968*, 171914.
29. R. Spurr; H. Myers; *Analytical Chemistry,* **1957**, *29*, 760-762.
30. D. Mardare; A. Manole; A. Yildiz; D. Luca; *Chem. Eng. Comm.*, **2011**, *198*, 530-540.